# Fermi-liquid behavior and thermal conductivity of $\epsilon$-iron at Earth's core conditions

L. V. Pourovskii[1,3], J. Mravlje[2], A. Georges[3,1,4], S.I. Simak[5], I. A. Abrikosov[5,6]
[1] *Centre de Physique Théorique, Ecole Polytechnique, CNRS, Université Paris-Saclay, F-91128 Palaiseau, France*
[2] *Jozef Stefan Institute, SI-1000, Ljubljana, Slovenija*
[3] *Collège de France, 11 place Marcelin Berthelot, 75005 Paris, France*
[4] *Department of Quantum Matter Physics, University of Geneva, 24 Quai Ernest-Ansermet, 1211 Geneva 4, Switzerland*
[5] *Department of Physics, Chemistry and Biology (IFM), Linköping University, SE-58183 Linköping, Sweden*
[6] *Materials Modeling and Development Laboratory, National University of Science and Technology "MISIS", Moscow, Russia*
(Dated: September 17, 2018)

The electronic state and transport properties of hot dense iron are of the utmost importance to geophysics. Combining the density functional and dynamical mean field theories we study the impact of electron correlations on electrical and thermal resistivity of hexagonal close-packed $\epsilon$-Fe at Earth's core conditions. $\epsilon$-Fe is found to behave as a nearly perfect Fermi liquid. The quadratic dependence of the scattering rate in Fermi liquids leads to a modification of the Wiedemann-Franz law with suppression of the thermal conductivity as compared to the electrical one. This significantly increases the electron-electron thermal resistivity which is found to be of comparable magnitude to the electron-phonon one. The implications of this effect on the dynamics of Earth's core is discussed.

arXiv:1603.02287v3 [cond-mat.str-el] 23 May 2016

Earth's magnetic field plays a crucial role in the survival of the human race. It keeps the ozone layer intact despite the solar wind and therefore protects the Earth from destructive ultraviolet radiation[1]. The magnetic field is generated by self-sustained dynamo action in its iron-rich core[2]. This geodynamo runs on heat from the growing solid inner core and on chemical convection provided by light elements issued from the liquid outer core on solidification[3]. The power supplied to drive the geodynamo is proportional to the rate of inner core growth, which in turn is controlled by heat flow at the core-mantle boundary[4]. This heat flow critically depends on the thermal and electrical conductivities of liquid iron under the extreme pressure and temperature conditions in the Earth's core. For a long time there has been agreement that convection in the liquid outer core provides most of the energy for the geodynamo and does so for at least 3.4 billion years[2, 5].

Recently, such a view has been challenged by first-principles calculations[3, 6], suggesting a much higher capacity for the liquid core to transport heat by conduction and therefore less ability to transport heat by convection[2]. The calculated conductivities have been found to be two to three times higher than the generally accepted estimates, urging for reassessment of the core thermal history and power requirements[3].

Convection also plays a crucial role in the current theory of the solid core dynamics, as a radial motion of the inner core matter is invoked to explain the observed seismic anisotropies of the inner core[7–9]. However, *ab initio* calculations[10] similarly predict a too high thermal conductivity for hexagonal close-packed (hcp) $\epsilon$-iron generally assumed to form the inner core, thus impeding a significant convection of its solid matter. The first-principles calculations for liquid and solid iron of Refs.[3, 6, 10], unlike previous results, have not relied on any extrapolations, however, they employed the standard density-functional-theory (DFT) framework in which dynamical many-body effects are neglected.

Many-body effects in crystalline iron at the conditions of Earth's inner core have been previously studied in Refs. [11, 12] using the density functional theory plus dynamical mean-field theory (DFT+DMFT) method[13, 14]. The hcp $\epsilon$-phase was predicted to exhibit a typical Fermi liquid behavior with a quadratic temperature dependence of the electron-electron scattering rate, $\Gamma$. In contrast, the body-centered cubic (bcc) $\alpha$-phase at the same conditions was shown to feature a strongly non-Fermi-liquid electron-electron scattering.

Zhang et al.[16] have later pointed out that the effect of electron-electron scattering (EES) of $d$-electrons due to correlations is missing in previous transport calculations within DFT [3, 10] and treatment of electron-phonon scattering (EPS) only is not sufficient. Using the same DFT+DMFT method they predicted a non-Fermi-liquid linear temperature dependence of the ESS in compressed $\epsilon$-iron, in disagreement with the conclusions of Ref. [11]. The EES contribution to the electrical resistivity at core temperatures was predicted to be as large as the electron-phonon one [16]. This principal result was later retracted [17] because of a numerical mistake in their transport calculations leading to a significant overestimation of the EES electrical resistivity.

Obviously, it is of the utmost importance to Earth's physics to clearly elucidate how large the EES contribution to the electrical and thermal resistivity at Earth's core conditions is. This is the motivation and the main subject of the present letter. We perform a detailed and

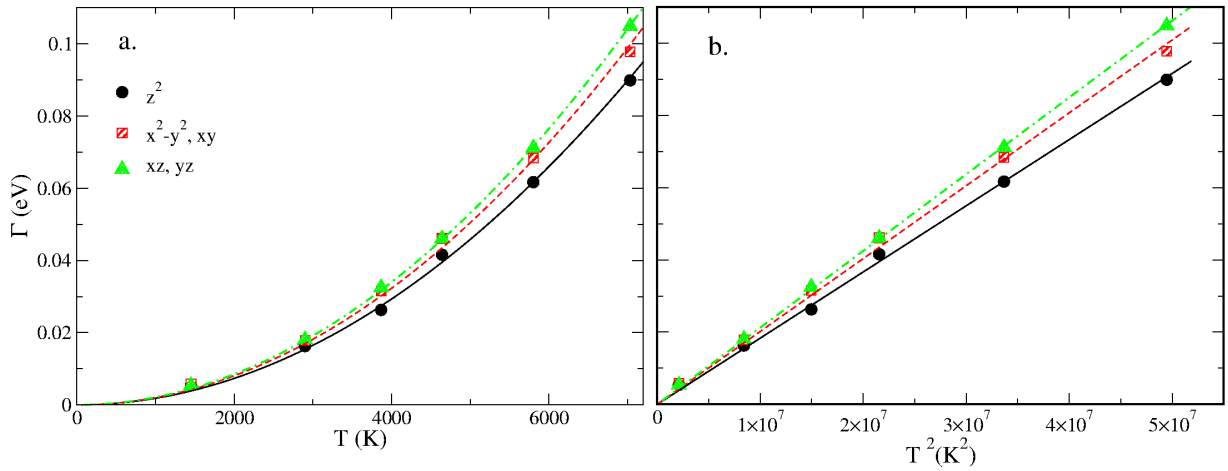


FIG. 1: (Color online) Orbitally-resolved values of the inverse quasi-particle lifetime Γ in $\epsilon$-Fe as a function of temperature T. a. Γ vs. $T$. The curves are fits $AT^2$ to the calculated data. b. Γ vs. $T^2$. The curves are linear-regression fits to the data. The values of Γ were extracted from real-axis self-energies obtained by the Maximum-entropy method [15].

precise calculation of the quasiparticle (QP) properties, especially of the QP scattering rate, and establish the FL nature of $\epsilon$-iron at the inner core conditions. Most importantly, the quadratic frequency dependence of the scattering rate characteristic of Fermi liquids has a direct bearing on the transport properties of $\epsilon$-Fe, as demonstrated here by an explicit calculation of the electrical and thermal conductivity. In Fermi liquids, the Lorenz number in the Wiedemann-Franz law is suppressed, thus the EES contribution to the thermal resistivity is enhanced. The EES contribution to the thermal resistivity is of comparable magnitude to the EPS one and should not be neglected. By including both contributions we obtain a substantially reduced value for the total thermal conductivity of pure $\epsilon$-Fe at the inner core conditions as compared to previous DFT calculations[10]. Hence, the Fermi-liquid nature of $\epsilon$-Fe suppresses its thermal conductivity and may play an important role in stabilizing the convection in the Earth core.

We employed the self-consistent DFT+DMFT implementation[18–20] in a full-potential framework[21]. We used the same parameters as in Ref. [11] for the lattice (volume 7.05 Å$^3$/atom, the hcp c/a ratio 1.6) and construction of the Wannier orbitals (energy window [10.8 eV, 4.0 eV] around the Fermi level), as well as around-mean-field double counting. The rotationally-invariant Coulomb interaction was defined by the parameters F0=U=5.0 eV and J=0.93 eV. The DMFT quantum impurity problem was solved using the hybridization-expansion continuous-time quantum Monte-Carlo method[22] as implemented in Ref. [23]. The same parameters were used for both hcp and bcc Fe. For the analytical continuation we employed the Maximum-entropy (MaxEnt) method in the implementation of Ref. [15]. The conductivity was calculated as described in Refs. [20] and [24].

First we analyze the temperature dependence of the inverse quasiparticle life-time $\Gamma_m = -Z_m Im[\Sigma_m(\omega = 0)]$, where $\Sigma_m(\omega = 0)$ is the value of DMFT self-energy for the orbital $m$ at zero frequency, $Z_m$ is the corresponding quasi-particle residue, $Z_m = \left(1 - \frac{dRe[\Sigma_m(\omega)]}{d\omega}\Big|_{\omega\to 0}\right)^{-1}$. Our resulting dependence of Γ vs. $T$ is plotted in Fig. 1a One may notice a clearly parabolic Fermi-liquid shape of $\Gamma(T)$ for all three inequivalent orbitals of the $3d$ shell of Fe in the hcp lattice. Correspondingly, Γ scales linearly as a function of $T^2$, see Fig. 1b. In contrast, the values of Γ obtained by Zhang et al. [16] exhibit a non-Fermi-liquid linear dependence on $T$. While our values agree with theirs at T=6000 K, for lower T the difference is significant. To obtain Γ plotted in Fig. 1 we have analytically continued the imaginary-frequency DMFT self-energy $\Sigma(i\omega_n)$, where $\omega_n$ is the fermionic Matsubara frequency $\omega_n = \pi(2n-1)k_B T$ and $k_B$ is the Boltzmann constant, to the real-frequency axis using the MaxEnt.

Our results for the scattering rate Γ shown in Fig. 1 are obtained from analytically-continued DMFT self-energy. It is well known that the analytical continuation methods needed to obtain the real-frequency data from the imaginary-frequency self-energy are quite sensitive to the details of the procedure (e.g. the number of Matsubara frequencies included into the Pade approximant[27], the way high frequency noisy tails are treated and the way the stochastic error is estimated in the initial imaginary-time data in the case of the MaxEnt etc.). However, a qualitative but definite conclusion about the Fermi or non-Fermi-liquid nature of a system can be inferred directly from the imaginary-frequency self-energy without resorting to any analytical continuation. This is done

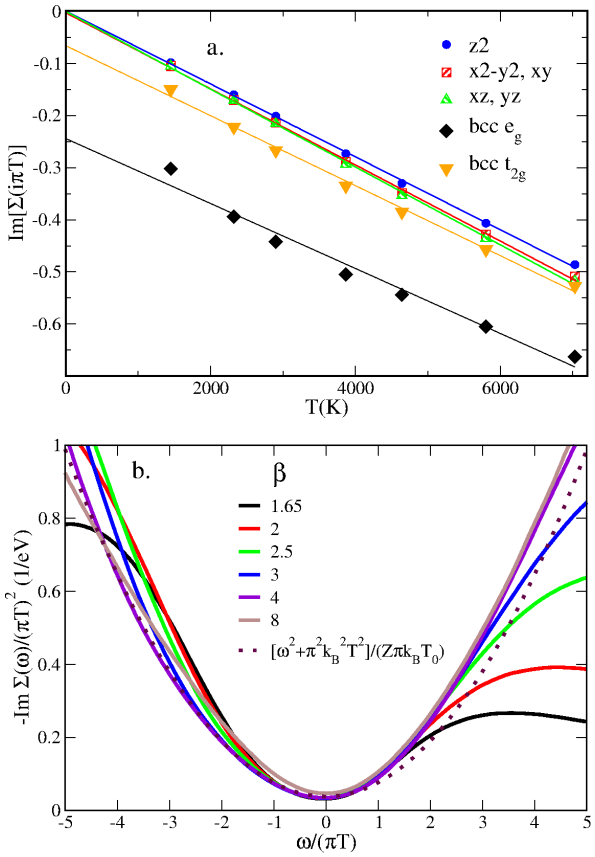


FIG. 2: (Color online) Fermi-liquid scaling of the DMFT self-energy in $\epsilon$-Fe. a. The imaginary part of the DMFT self-energy at the first Matsubara point $\omega_1 = i\pi k_B T$ vs. temperature for hcp and bcc Fe. Note that $Im[\Sigma(i\pi k_B T)]$ being proportional to T is a signature of a Fermi-liquid[25] . The lines are the linear regression fits to the calculated points for corresponding $3d$ orbitals of Fe. b. The rescaled imaginary part of the DMFT self-energy at the real axis, $Im[\Sigma(\omega)]/(\pi k_B T)^2$ , vs. $\omega/(\pi k_B T)$. The real-frequency self-energies are obtained by the MaxEnt analytic continuation method[15]. One sees that all self-energies collapse into a single curve described by a parabolic fit (the dotted line) defined by the quasiparticle weight $Z$ =0.7 and the characteristic Fermi-liquid temperature scale $T_0$ =12 eV. Deviations from the Fermi-liquid behavior of the resistivity are expected for temperatures above $T_{FL}$ ∼0.1 $T_0$ , see Ref. [26], i.e. $T_{FL}$ corresponds to about 14 000 K in the present case.

by employing the so-called "first-Matsubara-frequency" rule. As demonstrated, e. g., in Ref. [25], in a Fermi liquid the imaginary part of electronic self-energy, $\Sigma$, at the first Matsubara point within a local approximation like DMFT must be proportional to the temperature, T, i.e. $Im[\Sigma(i\pi k_B T)] = \lambda T$, where $\lambda$ is a real constant. In Fig. 2a we plot $Im[\Sigma(i\pi k_B T)]$ as a function of temperature for all inequivalent orbitals in hcp and bcc Fe. One may clearly see that in the $\epsilon$ phase $Im[\Sigma(i\pi k_B T)]$ is almost perfectly proportional to T, in contrast to bcc Fe, where it exhibits significant deviations from the "first-Matsubara-frequency" rule[11]. This result confirms the Fermi-liquid state of $\epsilon$-Fe at Earth's core conditions. We note that this conclusion is further corroborated by a weak temperature dependence of the of our calculated quasiparticle weight $Z$, as well as by the ratio $\frac{\Gamma}{T} \ll 1$.

Moreover, our real-frequency self-energies for different temperatures collapse into a curve consistent with the dependence $const \cdot (\omega^2 + (\pi k_B T)^2)$ expected for a Fermi liquid, see Fig. 2b . From this plot we extracted the upper bound $T_{FL}$ for the Fermi-liquid regime of the transport following Ref. [26]. The obtained temperature $T_{FL} \approx$ 14000 K is much higher than temperatures expected for Earth's core.

Fig. 3a shows our calculated contribution of the electron-electron scattering to the electrical resistivity. One clearly observes that it increases quadratically with increasing temperature up to at least 6000 K, corresponding to Earths core conditions, in contrast to the results of Ref. [16]. The obtained value of about 1.6·$10^{-5}$ Ω·cm at T=6000 K is rather insignificant compared to the electron-phonon-scattering contribution of about 5.3·$10^{-5}$ Ω·cm predicted by DFT calculations [10] indicating that the electron-electron scattering cannot strongly influence the electrical resistivity in hcp-Fe at Earth's core conditions.

In Fig. 3b we display the corresponding thermal conductivity due to electron-electron scattering. One may notice that this conductivity is not very high: its average magnitude of 540 $\mathrm{Wm^{-1}K^{-1}}$ at 6000 K is comparable to the figure ∼ 300 $\mathrm{Wm^{-1}K^{-1}}$ obtained in Ref. [10] for the electron-phonon thermal conductivity. By including both scattering effects the total conductivity is reduced to about 190 $\mathrm{Wm^{-1}K^{-1}}$, hence, the corresponding resistivity is enhanced by about 60%.

In fact, this large electron-electron-scattering contribution is directly related to the Fermi-liquid behavior of $\epsilon$-Fe. One may demonstrate this by simple analytical calculations [29–31]. Using a Fermi-liquid scattering rate $1/\tau(\omega) = 1/\tau_0 \cdot \left[1 + \omega^2/(\pi k_B T)^2\right]$ (with $1/\tau_0 \propto T^2$), the electrical conductivity ($\sigma$) and thermal conductivity ($\kappa$) are found to be, in the low-temperature limit $T \lesssim T_{FL}$ [31]:

$$\frac{\sigma}{\sigma_0} = \frac{I_{01}}{I_{00}} \simeq 0.82 \ , \ \frac{\kappa}{\kappa_0} = \frac{I_{21}}{I_{20}} \simeq 0.53 \qquad (1)$$

in which $\sigma_0$ and $\kappa_0$ denote the conductivities obtained with the frequency-independent scattering time $\tau_0$. In these expressions, $I_{nk} \equiv \int_{-\infty}^{+\infty} dx\, x^n (1 + x^2/\pi^2)^{-k} \cosh^{-2}(x/2)$ are transport integrals and $x = \omega/T$. Hence, the Lorenz number for such a Fermi-liquid with inelastic scattering only is equal to [29, 30]:

$$\frac{\kappa/T}{\sigma} = L_{FL} = L_0/1.54$$

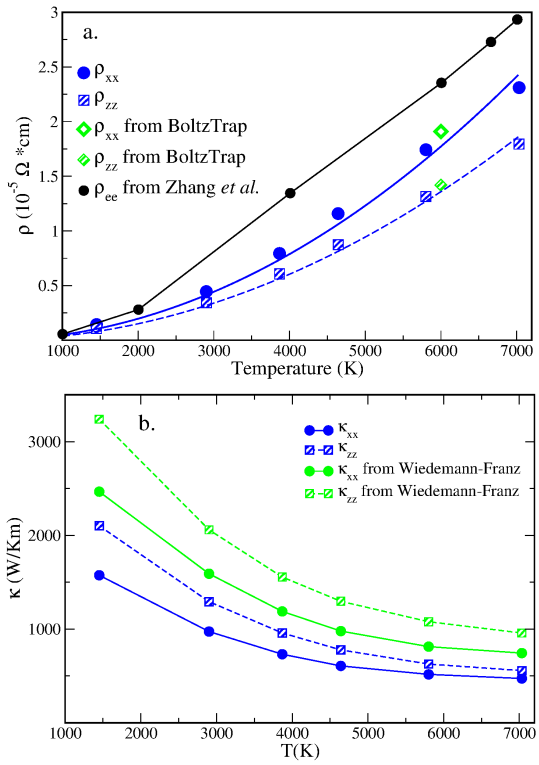


FIG. 3: (Color online)Calculated electron-electron-scattering contribution to the electrical and thermal resistivity of hcp iron at Earth's core density. a. Electrical resistivity. Blue filled circles and hashed squares are our DFT+DMFT results for $\rho_{xx}$ and $\rho_{zz}$ , respectively. Red filled and hashed triangles are the corresponding resistivities calculated by us with the imaginary part of the self-energy from Extended Data Fig. 3 of Zhang et al. [16]. Green empty and hashed diamonds are the corresponding resistivities calculated by the Boltzmann-transport code BoltzTrap [28] assuming a Fermi-liquid with $\Gamma/Z$ =0.09 eV. Black circles are the electron-electron-scattering contribution to the electrical resistivity reported obtained Zhang et al. [16] including the correction for the omitted spin factor [17]. b. Thermal conductivity. Blue filled circles and hashed squares are DFT+DMFT results for $\kappa_{xx}$ and $\kappa_{zz}$, respectively. The green lines/symbols are the corresponding conductivities obtained from our calculated electrical conductivity using the Wiedemann-Franz law with the standard Lorenz number of $2.44{\cdot}10^{-8}$ W$\Omega$K$^{-2}$.

where $L_0 = \pi^2/3(k_B/e)^2$ is the conventional Lorenz number for a frequency-independent scattering rate. The stronger effect of the frequency-dependence of $\tau(\omega)$ on the thermal conductivity as compared to $\sigma$ is due to the additional power $x^2$ in the numerator of the transport integrals for $\kappa$. Using the conventional value $L_0$ of the Lorenz number together with our calculated $\sigma$ would lead one to a substantially larger thermal conductivity (see Fig. 3b), and hence an incorrect conclusion that the electron-electron contribution to the thermal scattering is insignificant, too. This calculation can be generalized to take into account other sources of scattering on top of purely inelastic EES, such as impurity or electron-phonon scattering, leading to a $T$-dependent Lorenz number, as detailed in the supplemental material.

In conclusion, we have established $\epsilon$- iron is a Fermi liquid at Earth's core conditions. We have shown that implications of this finding are far reaching as the electron-electron inelastic scattering characteristic of Fermi-liquids significantly suppresses the thermal conductivity of Earth's inner core. The quadratic frequency dependence of this scattering leads to a reduction of the Lorenz number, hence, the thermal conductivity is suppressed with respect to predictions of the conventional Wiedemann-Franz law. As a result, the electron-electron-scattering contribution is comparable to the electron-phonon one. By taking them both into account, we obtained a significant reduction of the thermal conductivity of the $\epsilon$ phase at the inner core's condition, which supports explanations of the inner core anisotropy in terms of convection processes.

The same effects may be important for liquid iron, too. The obtained reduction is insufficient to explain the stability of convection by itself. But it is likely that the thermal disorder and the admixture of significant quantities of light elements [32], that we did not take into account may further decrease the thermal conductivity. The impact of alloying, crystalline order and thermal vibrations on electronic correlations should be investigated in future work. Finally, we note that the long-wave length spin-fluctuations that are disregarded in our approach may lead to additional suppression of the Lorenz number [33].

*Acknowledgments* L.V. P. acknowledges the financial support of the Ministry of Education and Science of the Russian Federation in the framework of Increase Competitiveness Program of NUST MISiS (No. K3-2015-038). J. M. is supported by the Slovenian Research Agency (ARRS) under Program P1-0044. A.G., J.M. and L.P. acknowledge the support of the European Research Council grant ERC-319286 QMAC. S.I.S. and I.A.A. acknowledge the Swedish Research Council (VR) Projects No. 2014-4750 and 2015-04391, LiLi-NFM, and the Swedish Government Strategic Research Area in Materials Science on Functional Materials at Linköping University (Faculty Grant SFO-Mat-LiU No. 2009 00971). I.A.A. is grateful for the support provided by the Swedish Foundation for Strategic Research (SSF) program SRL Grant No. 10-0026, as well as by the Ministry of Education and Science of the Russian Federation (Grant No. 14.Y26.31.0005). The computations were performed on resources provided by CPHT-Ecole Polytechnique as well as by the Swedish National Infrastructure for Computing (SNIC) at National Supercomputer Centre (NSC) and Center for High Performance Computing (PDC).

[1] J. A. Tarduno, R. D. Cottrell, W. J. Davis, F. Nimmo, and R. K. Bono, Science **349**, 521 (2015).
[2] P. Olson, Science **342**, 431 (2013).
[3] M. Pozzo, C. Davies, D. Gubbins, and D. Alfè, Nature **485**, 355 (2012).
[4] T. Lay, J. Hernlund, and B. Buffett, Nature Geosci. **1**, 25 (2008).
[5] F. Stacey and D. Loper, Physics of the Earth and Planetary Interiors **161**, 13 (2007).
[6] N. de Koker, G. Steinle-Neumann, and V. Vlček, Proc. Natl. Acad. Sci. U. S. A. **109**, 4070 (2012).
[7] B. Romanowicz, X.-D. Li, and J. Durek, Science **274**, 963 (1996).
[8] B. A. Buffett, Geophysical Journal International **179**, 711 (2009).
[9] M. Monnereau, M. Calvet, L. Margerin, and A. Souriau, Science **328**, 1014 (2010).
[10] M. Pozzo, C. Davies, D. Gubbins, and D. Alfè, Earth and Planetary Science Letters **393**, 159 (2014).
[11] L. V. Pourovskii, T. Miyake, S. I. Simak, A. V. Ruban, L. Dubrovinsky, and I. A. Abrikosov, Physical Review B **87**, 115130 (2013).
[12] O. Y. Vekilova, L. V. Pourovskii, I. A. Abrikosov, and S. I. Simak, Phys. Rev. B **91**, 245116 (2015).
[13] A. Georges, G. Kotliar, W. Krauth, and M. J. Rozenberg, Reviews of Modern Physics **68**, 13 (1996).
[14] G. Kotliar, S. Y. Savrasov, K. Haule, V. S. Oudovenko, O. Parcollet, and C. Marianetti, Reviews of Modern Physics **78**, 865 (2006).
[15] K. S. D. Beach, cond-mat/0403055.
[16] P. Zhang, R. Cohen, and K. Haule, Nature (London) **517**, 605 (2015).
[17] P. Zhang, R. Cohen, and K. Haule, Nature (London) (2016).
[18] M. Aichhorn, L. V. Pourovskii, V. Vildosola, M. Ferrero, O. Parcollet, T. Miyake, A. Georges, and S. Biermann, Phys. Rev. B **80**, 085101 (2009).
[19] M. Aichhorn, L. V. Pourovskii, and A. Georges, Phys. Rev. B **84**, 054529 (2011).
[20] M. Aichhorn, L. Pourovskii, P. Seth, V. Vildosola, M. Zingl, O. E. Peil, X. Deng, J. Mravlje, G. J. Kraberger, C. Martins, et al., Computer Physics Communications pp. – (2016).
[21] P. Blaha, K. Schwarz, G. Madsen, D. Kvasnicka, and J. Luitz, An augmented plane wave+ local orbitals program for calculating crystal properties (2001).
[22] E. Gull, A. J. Millis, A. I. Lichtenstein, A. N. Rubtsov, M. Troyer, and P. Werner, Rev. Mod. Phys. **83**, 349 (2011).
[23] P. Seth, I. Krivenko, M. Ferrero, and O. Parcollet, Computer Physics Communications **200**, 274 (2016).
[24] L. V. Pourovskii, J. Mravlje, M. Ferrero, O. Parcollet, and I. A. Abrikosov, Physical Review B **90**, 155120 (2014).
[25] A. V. Chubukov and D. L. Maslov, Phys. Rev. B **86**, 155136 (2012).
[26] C. Berthod, J. Mravlje, X. Deng, R. Žitko, D. van der Marel, and A. Georges, Phys. Rev. B **87**, 115109 (2013).
[27] K. S. D. Beach, R. J. Gooding, and F. Marsiglio, Phys. Rev. B **61**, 5147 (2000).
[28] G. K. Madsen and D. J. Singh, Computer Physics Communications **175**, 67 (2006).
[29] C. Herring, Phys. Rev. Lett. **19**, 167 (1967).
[30] C. Herring, Phys. Rev. Lett. **19**, 684 (1967).
[31] See Supplemental Material at XXXXX for a detailed derivation of the Lorentz number for Fermi liquids and calculations within the Boltzmann approach.
[32] J. G. O'Rourke and D. J. Stevenson, Nature (London) **529**, 387 (2016).
[33] A. I. Schindler and M. J. Rice, Phys. Rev. **164**, 759 (1967).
[34] N. Ashcroft and N. D. Mermin, *Solid state physics.* (Brooks Cole, 1976), chap. 7.

# Supplemental material

In a standard Boltzmann formalism within the relaxation time approximation the conductivity ($\sigma$) and the thermal conductivity ($\kappa$) are given as specified, e.g., in Ref. [34]:

$$\sigma = e^2 \int d\epsilon \Phi(\epsilon)(-f'(\epsilon))\tau(\epsilon), \tag{S1}$$

$$\kappa = \frac{1}{T}\int d\epsilon^2 \Phi(\epsilon)(-f'(\epsilon))\tau(\epsilon) - \frac{\left[\int d\epsilon\epsilon\Phi(\epsilon)(-f'(\epsilon))\tau(\epsilon)\right]^2}{\int d\epsilon\Phi(\epsilon)(-f'(\epsilon))\tau(\epsilon)} \tag{S2}$$

where $\epsilon$ is the energy measured with respect to the chemical potential, $\Phi(\epsilon)$ is the transport function, $f$ is the Fermi function and $\tau$ is the relaxation time. Often the energy dependence of $\tau$ is neglected. If one additionally neglects the energy dependence of transport function and evaluates the elementary integrals, one gets the Wiedemann-Franz law

$$\kappa/(\sigma T) = \frac{\pi^2}{3}\left(\frac{k_B}{e}\right)^2 = L,$$

where the Lorenz number $L$ is $2.44{\cdot}10^{-8}\mathrm{W\Omega K^{-2}}$.

In the case of a Fermi liquid, however, the energy dependence of scattering rate is very strong

$$1/\tau(\epsilon) = 1/\tau(\epsilon = 0)\cdot(1 + \epsilon^2/(\pi T k_B)^2)$$

This leads to a modification of the Wiedemann-Franz law

$$\kappa/(\sigma T) = L/1.54 = L_{FL}$$

Accordingly, the conductivity and thermal conductivity from Eqs. S1 and S2 will be smaller by 0.82 and 0.53, respectively, if compared with that obtained by neglecting the energy dependence of the scattering rate, i.e. by putting

$$1/\tau(\epsilon) = 1/\tau(\epsilon = 0)$$

into Eqs. S1 and S2 .

Remarkable suppression of the thermal conductivity is especially important for the discussion in the main text.

One may estimate the impact of this effect on the overall thermal conductivity of $\epsilon$-Fe by summing up the contributions from electron-electron and electron-phonon scattering. To obtain the later we evaluated the ratio $\kappa/\tau$ using the BoltzTraP[28] code. By adopting for the conductivity with electron-phonon scattering, $\kappa_{e-ph}$ , the value of 300 $\mathrm{Wm^{-1}K^{-1}}$ obtained by DFT calculations of Ref. [10] , we estimated the electron-phonon quasiparticle lifetime $\tau_{e-ph}$ =$1.11{\cdot}10^{-15}$ s. Assuming a frequency-independent electron-phonon scattering one obtains for the total lifetime :

$$\frac{1}{\tau_{tot}} = \frac{1}{\tau_{e-ph}}\left[1 + \frac{\tau_{e-ph}}{\tau(\epsilon = 0)}(1 + \epsilon^2/(\pi T k_B)^2)\right].$$

The electron-electron scattering contribution to the thermal conductivity evaluated with full DMFT transport calculations is shown in Fig. 3b of the main text. Here we present a simple semi-classical calculations, where electron-electron-scattering lifetime is obtained from the average value of self-energy at zero frequency, 0.09 eV. Hence, $\tau(\epsilon = 0) = \hbar/(2\Sigma(0))$ is $3.66{\cdot}10^{-15}$ s and the ratio $\tau_{e-ph}/\tau(\epsilon = 0)$=0.303. Inserting $\tau_{tot}$ into (S2) and carrying out the integration assuming a constant value for the transport function one obtains the reduction of $\kappa$ by a factor of 0.61 as compared to pure electron-phonon scattering. Hence, the thermal conductivity is reduced from 300 to 183 $\mathrm{Wm^{-1}K^{-1}}$. This value is very close to the one obtained by adding the electron-electron thermal scattering calculated directly within DMFT (Fig 3.b of the main text) to the electron-phonon contribution, $\kappa_{tot} = 1/(\kappa_{e-e}^{-1} + \kappa_{e-ph}^{-1})$ =190 $\mathrm{Wm^{-1}K^{-1}}$.

The Lorenz number depends on the magnitude of the electron-electron scattering compared to that of the other scattering processes. As an illustration of this, we consider elastic, temperature independent scattering whose magnitude we set to the $\tau_{e-ph}$ at 6000 K and plot the Lorentz number as a function of temperature in Fig.S1. At high temperatures the electron-electron scattering that in a Fermi liquid increases quadratically with temperature dominates and the Lorentz number approaches the pure Fermi liquid result of 2.14 $(k_B/e)^2$. At low temperatures the electron-electron scattering is insignifcant and standard Lorenz number of $\pi^2/3(k_B/e)^2$ is recovered instead.

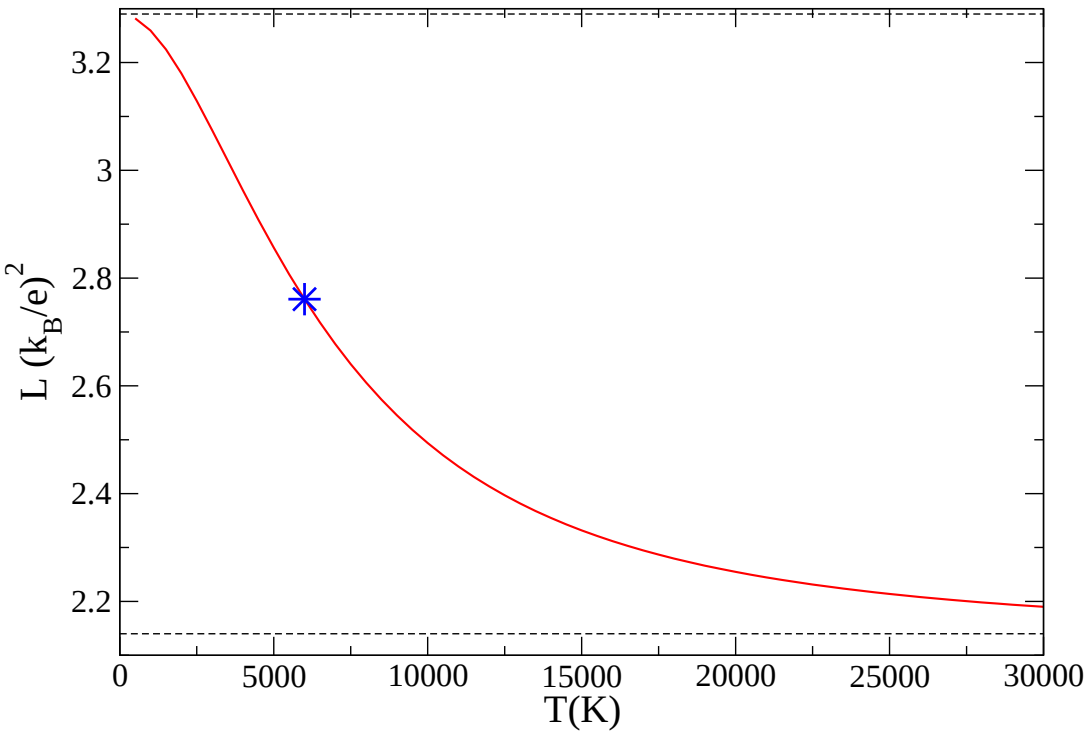


FIG. S1: The Lorenz number vs. temperature. The star indicates the value of $L$ at the inner core temperature of 6000 K.